ACI MATERIALS JOURNAL TECHNICAL PAPER

Title no. 107-M34

Performance of Permeability-Reducing Admixtures in Marine Concrete Structures

by Vinh T. N. Dao, Peter F. Dux, Peter H. Morris, and Alan H. Carse

The use of permeability-reducing admixtures is a potential preventative of the chloride-induced corrosion of steel reinforcement, which is the main cause of the deterioration of concrete structures exposed to coastal environments. This paper presents an experimental investigation into the effectiveness of two typical commercially available permeability-reducing admixtures: one characterized by crystallization activity and the other by hydrophobic and pore-blocking effects. Concrete specimens were exposed to simulated coastal environments, and chloride concentration profiles at 28-, 365-, and 730-day exposures were determined by X-ray fluorescence spectrometry. The results suggested that the incorporation of the admixture, characterized by hydrophobic and pore-blocking effects, appeared to considerably enhance the concrete durability with respect to chloride-induced corrosion. The inclusion of the admixture characterized by crystallization activity, however, seemed to have almost no detectable effect. This implies the necessity of exercising a degree of caution during specification.

Keywords: chloride-induced corrosion; coastal environment; durability; permeability-reducing admixture.

INTRODUCTION

Chloride-induced corrosion of steel reinforcement is a well-known and well-documented phenomenon, and is considered to be the main cause of deterioration of reinforced concrete structures exposed to coastal environments.[1,2] The traditional means of improving concrete durability with respect to chloride-induced corrosion are to ensure high-quality concrete and adequate cover. Other measures include the use of cathodic protection, epoxy-coated and stainless-steel reinforcement, corrosion inhibitors, penetrating sealers, and waterproofing membranes.[1,3]

Permeability-reducing admixtures, a potential solution to the problem of corrosion deterioration of structures, have been researched and introduced into service.[4] They are claimed by their manufacturers to greatly reduce water penetration as well as to enhance other properties of concrete; however, the performance of these commercial products in concrete structures exposed to coastal environments has yet to be confirmed, especially with regard to chloride-induced corrosion.

The objective of this study was to experimentally investigate the effectiveness of two typical internationally commercially available permeability-reducing admixtures in improving the chloride penetration characteristics of concrete exposed to simulated coastal environments. The two admixtures were characterized by: 1) crystallization activity, and 2) hydrophobic and pore-blocking effects, respectively.

RESEARCH SIGNIFICANCE

The chloride-induced corrosion of steel reinforcement is the main cause of the deterioration of reinforced concrete structures exposed to coastal environments, which annually costs billions of dollars for the repair and maintenance of these structures. This paper presents the results of an investigation into the effectiveness of permeability-reducing admixtures in enhancing the durability of concrete structures against such chloride-induced corrosion. These results provide the basis for an informed choice of permeability-reducing admixtures and highlight the necessity of exercising caution during specification. Also, the realistic results obtained from the cyclic wetting-and-drying exposure of test specimens in this study, which are reasonably representative of concrete in the field, serve as valuable input for service life modeling of concrete structures exposed to coastal environments.

DESCRIPTION OF ADMIXTURES

The permeability-reducing admixture characterized by crystallization activity was supplied in powder form and consisted of portland cement and various active, proprietary chemicals. According to information supplied by the manufacturer, these chemicals react with the moisture in fresh concrete and with the by-products of cement hydration to generate an insoluble crystalline formation in the pores and capillary tracts that inhibits penetration by liquids.

The admixture characterized by hydrophobic and pore-blocking effects was supplied in aqueous form. According to the manufacturer's manual, the "hydrophobic" components change the surface tension of the cement hydrates and capillary surfaces, making them water-repellent[5,6]; and under water pressure, the "pore-blocking" components form physical plugs that block the capillaries. These actions result in a reduction in the permeability of the concrete.

EXPERIMENTAL PROCEDURES

The performance of the two admixtures was compared using three concrete mixtures with the target compressive strength at 28 days of 40 MPa (5.8 ksi). The three mixtures were denoted Control for the control mixture and "C" and "HPI" for the mixtures incorporating the permeability-reducing admixtures characterized by crystallization (C) activity and by hydrophobic and pore-blocking (HPI) effects, respectively. The dosage and mixing sequence of the admixtures conformed to the respective manufacturer's technical information. The manufacturers' technical representatives attended the mixing and casting of the specimens. The chemical compositions of fly ash and cement used are given in Fig. 1 and Table 1; and the three mixture designs are summarized in Table 2.

ACI Materials Journal, V. 107, No. 3, May-June 2010.
MS No. M-2009-206 received June 15, 2009, and reviewed under Institute publication policies. Pertinent discussion including authors' closure, if any, will be published in the March-April 2011 *ACI Materials Journal* if the discussion is received by December 1, 2010.

Vinh T. N. Dao *is a Lecturer in the School of Civil Engineering at the University of Queensland, Australia, where he received his MEng and PhD. His research interests include structures and concrete technology.*

Peter F. Dux *is a Professor and Head of the School of Civil Engineering at the University of Queensland, where he received his PhD. His research interests include structures and concrete technology.*

Peter H. Morris *is a Research Fellow in the School of Civil Engineering at the University of Queensland, where he received his PhD. His research interests include mobile-boundary hydraulics, geomechanics, the disposal of mine wastes and dredge spoil, and the behavior and properties of early-age and mature concrete.*

Alan H. Carse *(deceased) was Principal Engineer (Concrete Technology) in the Structures Division of Queensland Main Roads Department, Australia. He received his PhD from the University of Queensland, for research into alkali-silica reaction, a field in which he has achieved international recognition.*

The concretes tested were deliberately specified to enable sufficient and meaningful data to be obtained within the reasonable period of 2 years. The pertinent Australian standard[7] requires concrete members exposed to tidal or splash zones in sea water to have a minimum characteristic compressive strength at 28 days of 50 MPa (7.3 ksi).

The concrete was mixed in a laboratory rotary pan concrete mixer. The mixing water (Table 2) was based on the saturated surface-dry condition of the aggregates and was adjusted to achieve the desired slump in the actual mixtures. The mixing water used was 216.8, 204, and 165 L/m^3 (375.1, 352.9, and 285.5 in.^{3}/ft^3) for the Control, "C", and "HPI" mixtures, respectively. Because the "HPI" admixture was in liquid form, the actual mixing water for the "HPI" mixture was approximately 195 L/m^3 (337.4 in.^{3}/ft^3).

The mixing sequence used for the Control and "C" mixtures followed normal practice for ordinary concrete.

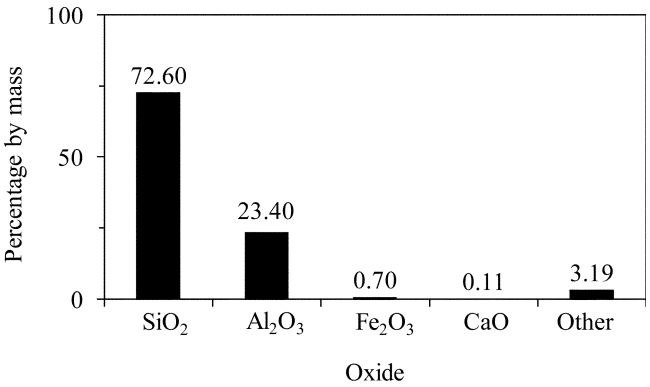

Fig. 1—Chemical analysis of fly ash.

Fig. 2—Experimental setup.

First, aggregates, cement, and fly ash (together with "C" powder in the case of the "C" mixture) were mixed. The target slump was 25 mm (1.0 in.) upon the addition of mixing water containing water-reducer. It was then increased to 75 mm (3.0 in.) by the addition of the high-range water-reducing admixture. The mixing sequence for the "HPI" mixture, following the manufacturer's advice, was different, with the mixing water and "HPI" admixture being introduced into the mixture before the aggregates, cement, and fly ash. A high-range water-reducing admixture was added at the end to bring the slump up to the target value.

Concrete of each mixture was cast into 350 mm (13.8 in.) square by 750 mm (29.5 in.) high reinforced columns with cover to the reinforcement of 50 mm (2.2 in.). The columns were cured in timber molds for 3 days, and then exposed to a simulated coastal environment in specimen tanks (Fig. 2). The level of simulated seawater in the specimen tanks rose and fell periodically (Fig. 3) to model real tidal conditions as water was pumped to and fro between the tanks and a reservoir tank. The cyclic wetting-and-drying exposure gave conditions that were reasonably representative of those experienced by concrete in the field and, hence, more realistic results.

The simulated tidal period was 12 hours, divided equally between rising and falling tides (Fig. 3). Seawater was simulated by dissolving 32.1 g (0.07 lb) of common salt per kilogram (2.2 lb) of water to match the typical chlorinity in Moreton Bay, Australia, of 19,500 ppm.[8] This was checked regularly using a salinity measurement device, and was adjusted as necessary to maintain constant conditions.

After the columns had been exposed for 28, 365, and 730 days to the simulated coastal conditions, concrete powder samples were taken by drilling (in 10 mm [0.4 in.] depth increments) and their total chloride contents were determined by X-ray fluorescence spectrometry. The data

Table 1—Cement batch sheet for general purpose portland cement

SiO_2	Al_2O_3	Fe_2O_3	CaO	MgO	SO_3	Loss on ignition
22.4%	4.8%	3.6%	67.4%	1.2%	2.3%	0.2%
C_3S	C_2S	C_3A	C_4AF	Free lime	Na_2O equivalent	
66%	14%	6.6%	11.0%	0.5%	0.41%	

Table 2—Summary of concrete mixture designs

Constituents	Unit	Control	C	HPI
Cement	kg/m^3	300	300	300
Fly ash	kg/m^3	100	100	100
Water	kg/m^3	176	176	155
Water reducer	L/m^3	1.2	1.2	—
"C" admixture	kg/m^3	—	4.0	—
"HPI" admixture	L/m^3	—	—	30
High-range water-reducing admixture	L/m^3	1.6	1.6	4.4
20 mm aggregate	kg/m^3	759	759	759
10 mm aggregate	kg/m^3	229	229	229
Coarse sand	kg/m^3	600	600	600
Fine sand	kg/m^3	176	176	176

Note: 1 in. = 25.4 mm; 1 lb/ft^3 = 16 kg/m^3; 1 in.^{3}/ft^3 = 0.578 L/m^3.

obtained were considered to be sufficient to enable the comparison of the relative performance of the mixtures, especially including the time to corrosion initiation, with acceptable certainty.

A 25 mm (1.0 in.) drill bit, larger than the maximum aggregate of 20 mm (0.8 in.), was used for all sampling to minimize the likelihood of a hole being drilled completely through a solid piece of aggregate and consequently giving an abnormally low value of chloride concentration.[9] The correct depths for powder sampling were checked using a simple depth gauge, and also by comparing the weights of the samples.

Concrete powder samples were collected at all depth increments from each column at three locations at heights of 80, 300, and 560 mm (3.1, 11.8, and 22.0 in.) from the base (Fig. 3), and were combined to give a representative sample of each depth increment. The three heights were chosen to represent the submerged zone, tidal zone, and high tide level, respectively (Fig. 3).

RESULTS AND DISCUSSION

The compressive strength and shrinkage of the concrete mixtures, determined in accordance with the relevant Australian standards, are plotted in Fig. 4 and 5. The strength developed almost identically in the Control and "C" mixtures, whereas that of "HPI" mixture was slightly slower (Fig. 4). The 28-day compressive strengths of the Control, "C," and "HPI" mixtures were 43.1, 43.0, and 38.8 MPa (6.3, 6.2, and 5.6 ksi), respectively. The development of shrinkage is similar in all three mixtures, although the shrinkage of the "C" mixture was slightly higher than those of the other two mixtures (Fig. 5).

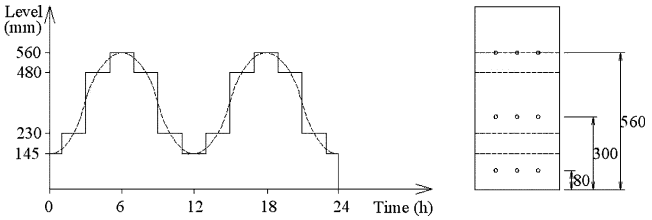

Fig. 3—Cycles of simulated tide and locations for concrete powder sampling. (Note: 1 in. = 25.4 mm.)

Based on the chloride profiles after 28 days of exposure, the background chloride concentration was taken as 0.2% by mass of cementitious material (equivalent to about 0.035% by mass of concrete). The measured total chloride concentrations after a subtraction of 0.2% background concentration expressed as percentage by mass of cementitious material, upon which all subsequent calculations were based, are presented in Table 3.

For unidirectional diffusion into a semi-infinite medium with a constant diffusion coefficient, a constant surface chloride concentration C_o, and the initial condition, $C_{(x,t)} = 0$ for $x > 0$,

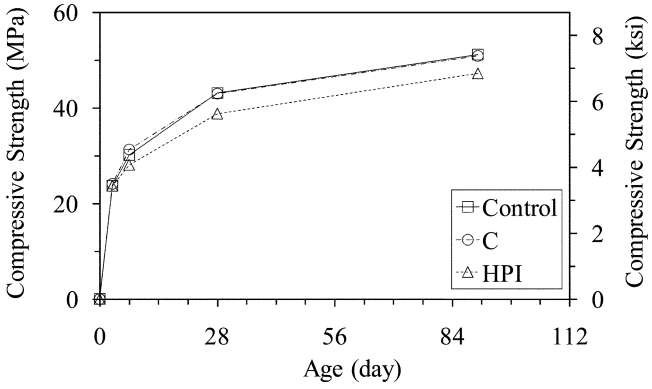

Fig. 4—Compressive strengths.

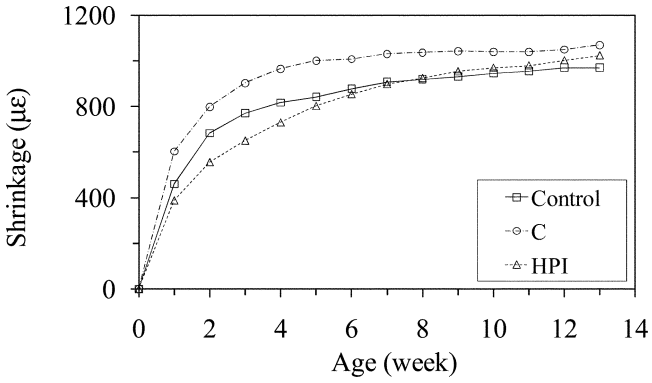

Fig. 5—Shrinkage.

Table 3—Measured total chloride concentrations

Height, mm	Depth, mm	28-day exposure			365-day exposure			730-day exposure		
		Control	C	HPI	Control	C	HPI	Control	C	HPI
80	0 to 10	3.08	3.30	0.63	4.09	4.79	1.10	4.63	4.25	1.28
	10 to 20	0.63	0.69	0.08	2.18	2.29	0.26	3.08	3.13	0.39
	20 to 30	0.11	0.11	0.06	0.52	0.81	0.09	1.23	0.99	0.10
	30 to 40	0.09	0.01	0.15	0.09	0.17	0.09	0.19	0.10	0.09
300	0 to 10	2.42	2.47	1.17	4.87	4.13	2.93	5.58	4.67	2.10
	10 to 20	0.46	0.57	0.07	2.12	2.00	0.69	3.67	2.47	0.80
	20 to 30	0.10	0.07	0.08	0.57	0.63	0.12	1.35	0.93	0.17
	30 to 40	0.03	0.04	0.07	0.08	0.14	0.11	0.25	0.14	0.07
560	0 to 10	2.00	2.06	1.04	7.55	6.33	5.12	7.55	7.52	4.59
	10 to 20	0.32	0.15	0.07	2.42	2.41	2.40	4.09	3.60	2.11
	20 to 30	0.07	0.03	0.10	0.46	0.63	0.51	1.17	0.93	0.86
	30 to 40	0.06	0.08	0.07	0.12	0.14	0.13	0.24	0.14	0.30

Note: 1 in. = 25.4 mm.

$t = 0$, the chloride concentration $C_{(x,t)}$ at depth x, and time t is given by[10-12]

$$C_{(x,t)} = C_o\left(1 - erf\left(\frac{x}{2\sqrt{Dt}}\right)\right) \quad (1)$$

where x is taken as the average for each depth increment (for example, 0.005 m [0.2 in.] for a sample taken between depths of 0 to 0.01 m [0.4 in.]); and *erf* is the standard error function

$$erf(x) = \frac{2}{\sqrt{\pi}}\int_0^x e^{-t^2}dt$$

Both the diffusion coefficient D and the surface concentration C_o for each concrete mixture at each age and height were determined by fitting Eq. (1) to the corresponding measured chloride profiles. The best fit was determined by adjusting both D and C_o to achieve the highest coefficient of determination, R^2, using a commercially available curve-fitting software program. The best-fit values are presented in Table 4. The estimated diffusion coefficients are consistent with those reported by other researchers[13-16] for similar concretes. The R^2 values were higher than 0.98 in. all cases with the sole exception of the "HPI" mixture at 28 days at the 80 mm (3.1 in.) level, giving a clear indication of good fits. It should be emphasized, however, that the values of D and C_o do not necessarily represent the actual chloride diffusion coefficient and surface chloride concentration; they are simply regression coefficients that are convenient to use to compare the performance of concretes with different qualities.

The diffusion coefficients in Table 4, which are plotted in Fig. 6, show that both D and its rate of decrease for each type of concrete decreased with time. The D for the 365-day exposure were approximately 65 to 85% lower than the corresponding 28-day values, whereas the 730-day values were approximately 3 to 40% lower than the corresponding 365-day values. The decrease of both D and its rate of decrease with time are probably mainly attributable to the early exposure of the concrete to simulated seawater (at the age of 3 days) and the continuing formation of hydration products and their effect on the pore system within the concrete.

The decrease of the diffusion coefficient with time, especially during the first year, should be recognized in estimating the time to corrosion initiation of reinforced concrete structures. As an illustration of this, the chloride profiles after 5 and 30 years of exposure for a concrete structure with a surface chloride concentration of 9.0% are plotted in Fig. 7 for diffusion coefficients varying between 2×10^{-12} m^2/seconds (3.1×10^{-9} in.^{2}/seconds) and 10×10^{-12} m^2/s (15.5×10^{-9} in.^{2}/seconds). It can be readily seen that the chloride concentrations at all depths after 5 years of exposure for a diffusion coefficient of

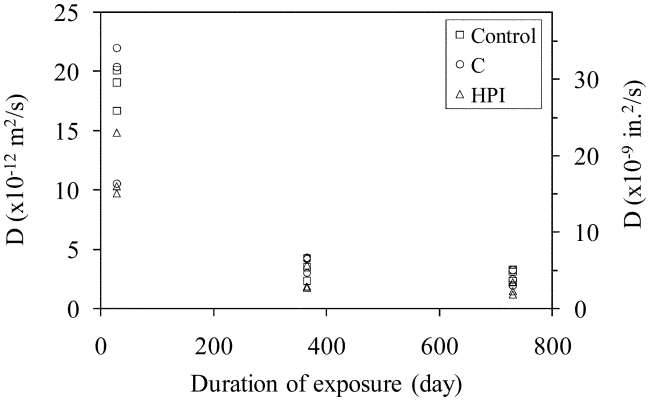

Fig. 6—Variation of diffusion coefficient with time.

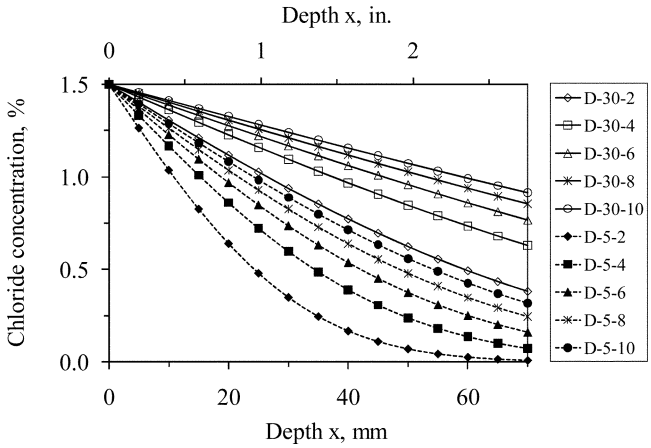

Fig. 7—Illustration of effect of diffusion coefficient on chloride concentration profile. (Note: "D-30-2" denotes case for diffusion coefficient of 2×10^{-12} m^2/seconds [3.1×10^{-9} in.^{2}/seconds] after 30 years.)

Table 4—Best-fit values of D, C_o, and corresponding R^2

Height	Best-fit values	28-day exposure			365-day exposure			730-day exposure		
		Control	C	HPI	Control	C	HPI	Control	C	HPI
80 mm (3.1 in.)	D	20.09	20.36	14.84	4.28	4.28	1.86	3.27	3.25	1.18
	C_o	5.03	5.37	1.13	5.46	6.30	1.70	5.93	5.57	1.87
	R^2	1.00	1.00	0.88	0.99	1.00	0.98	0.98	0.95	0.99
300 mm (11.8 in.)	D	19.04	21.99	9.72	3.50	4.18	1.74	3.14	2.45	1.46
	C_o	4.01	3.93	2.51	6.63	5.47	4.62	7.18	6.06	2.95
	R^2	1.00	1.00	0.99	1.00	1.00	1.00	0.98	1.00	1.00
560 mm (22.0 in.)	D	16.68	10.51	10.33	2.37	3.00	3.65	2.30	1.93	2.22
	C_o	3.46	4.26	2.17	11.06	8.83	6.96	9.95	10.12	5.96
	R^2	1.00	1.00	0.98	1.00	1.00	1.00	0.99	1.00	1.00

Note: D is expressed in 10^{-12} m^2/second (1.55×10^{-9} in.^{2}/second); and C_o is expressed as percentage by mass of cementitious material.

10×10^{-12} m^2/seconds (15.5×10^{-9} in.^{2}/seconds) are smaller than the corresponding concentrations for a diffusion coefficient of 2×10^{-12} m^2/seconds (3.1×10^{-9} in.^{2}/seconds) after 30 years of exposure. Given the large range of diffusion coefficients in Table 4, it is clear that caution should be exercised when estimating the service life of structures based on chloride profiles taken at any given time, especially during the first year of exposure.

To compare the relative performance of the three mixtures, the time to initiation of corrosion of the three concrete columns was estimated using the model of Mangat and Molloy,[17] in which D at a given time t can be expressed in the form

$$D = D_i t^{-m} \tag{2}$$

where D_i is the diffusion coefficient at a time t equal to 1 second, and m is an empirical coefficient. Substituting Eq. (2) in Eq. (1) gives

$$C_{(x,t)} = C_o\left(1 - erf\left(\frac{x}{2\sqrt{\frac{D_i}{1-m}t^{(1-m)}}}\right)\right) \tag{3}$$

To reflect the reality that the concrete at any given level on the three concrete columns was exposed to the same wetting and drying conditions, C_o was assumed to be constant for concrete at any particular level. Based on the best-fit values in Table 4, C_o was taken as 5, 6, and 10% for the concrete at the 80, 300, and 560 mm (3.1, 11.8, and 22.0 in.) levels, respectively (Fig. 3). The diffusion coefficient D was then determined by fitting Eq. (1) to the respective measured chloride profiles listed in Table 3. The coefficients D_i and m for each type of concrete at a given level were then estimated using Eq. (2). The resulting D, D_i, and m are presented in Table 5.

Assuming a chloride threshold concentration of 1.0% by mass of cementitious material[18-21] and a depth of cover to reinforcement of 50 mm (2.0 in.), the time to corrosion initiation, T, can be estimated using Eq. (3). The results are presented in Table 5. The generally short estimated time to initiation of corrosion (Table 5) was probably attributable mainly to the early exposure to the simulated coastal environments at the age of 3 days. Although this represents normal construction practice for many concrete structures, other structures experience better curing regimes and thus should have longer times to corrosion initiation. It should be emphasized that the estimated values are not necessarily a true representation of times to corrosion initiation; the values are only presented to allow a comparison to be made between different concretes.

Importantly, Table 5 shows that the "HPI" mixture had significantly longer estimated times to the initiation of corrosion than the "C" and Control mixtures at all levels. The time to initiation of corrosion of the "C" mixture was slightly longer than that of the Control mixture at the 300 and 560 mm (11.8 and 22.0 in.) levels, but slightly shorter at the 80 mm (3.1 in.) level. The incorporation of the admixture characterized by hydrophobic and pore-blocking effects in the "HPI" mixture thus appeared to considerably extend the time to the initiation of corrosion. The inclusion of the admixture characterized by crystallization activity, however, seemed to have no detectable effect on the time to the onset of corrosion.

SUMMARY AND CONCLUSIONS

The use of permeability-reducing admixtures in concrete mixtures as one of the solutions to chloride-induced corrosion of steel reinforcement in concrete structures previously lacked supporting data, prompting the study of their performance reported in this paper. The effectiveness of two typical commercially available permeability-reducing admixtures, one characterized by crystallization activity and the other by hydrophobic and pore-blocking effects, was studied experimentally.

Details of the materials and experimental procedures adopted in the study were presented. Experimental chloride concentrations of concrete specimens after 28-, 365-, and 730-day exposures to a simulated coastal environment that

Table 5—Estimated time *T* to initiation of corrosion

Height	Best-fit values	Control			C			HPI		
		28 days	365 days	730 days	28 days	365 days	730 days	28 days	365 days	730 days
80 mm (3.1 in.)	D	20.3	4.9	4.3	23.3	6.3	3.9	2.2	0.3	0.2
	C_o	5.0			5.0			5.0		
	D_i	39,172.9			55,296.3			443,010.0		
	m	0.515			0.529			0.831		
	T	3.4			2.6			3,846,599.0		
300 mm (11.8 in.)	D	7.8	4.1	3.9	8.3	3.5	2.5	3.1	1.0	0.2
	C_o	6.0			6.0			6.0		
	D_i	231.1			1469.0			10,509.5		
	m	0.230			0.352			0.553		
	T	4.4			6.5			193.7		
560 mm (22.0 in.)	D	3.2	2.8	2.3	3.2	2.4	2.0	2.0	1.7	0.6
	C_o	10.0			10.0			10.0		
	D_i	10.1			25.2			35.9		
	m	0.079			0.140			0.196		
	T	5.2			6.4			14.4		

Note: D and D_i is expressed in 10^{-12} m^2/second (1.55×10^{-9} in.^{2}/second); C_o is expressed as percentage by mass of cementitious material; and T is expressed in years.

were determined by X-ray fluorescence were reported. The diffusion coefficients and corresponding times to corrosion initiation were estimated based on Fick's second law of diffusion.

The incorporation of an admixture characterized by hydrophobic and pore-blocking effects appeared to considerably improve concrete durability with respect to chloride-induced corrosion, as shown by the reduced diffusion coefficient and longer estimated time to corrosion initiation. The inclusion of an admixture characterized by crystallization activity, however, seemed to have almost no detectable effects.

ACKNOWLEDGMENTS

The authors gratefully acknowledge the Queensland Main Roads Department for its financial support of this study.

REFERENCES

1. Broomfield, J. P., *Corrosion of Steel in Concrete: Understanding, Investigation and Repair*, E&FN Spon, London, UK, 1997, 240 pp.

2. Glass, G. K., and Buenfeld, N. R., "Chloride-Induced Corrosion of Steel in Concrete," *Progress in Structural Engineering and Materials*, V. 2, No. 4, 2000, pp. 448-458.

3. ACI Committee 222, "Design and Construction Practices to Mitigate Corrosion of Reinforcement in Concrete Structures (ACI 222.3R-03)," American Concrete Institute, Farmington Hills, MI, 2003, 29 pp.

4. Aldred, J. M., "The Relative Importance of Permeability and Sorptivity in the Corrosion of Reinforced Concrete," *Proceedings of the 5th Asian-Pacific Corrosion Control Conference & 27th Australasian Corrosion Association Conference*, Australasian Corrosion Association, Melbourne, Australia, 1987, pp. 1-8.

5. Aldred, J. M.; Swaddiwudhipong, S.; Lee, S. L.; and Wee, T. H., "The Effect of Initial Moisture Content on Water Transport in Concrete Containing a Hydrophobic Admixture," *Magazine of Concrete Research*, V. 53, No. 2, 2001, pp. 127-134.

6. Newman, J., and Choo, B. S., *Advanced Concrete Technology—Constituent Materials*, Butterworth-Heinemann, Oxford, 2003, 280 pp.

7. Standards Australia, "AS 3600-2001: Concrete Structures," 2001.

8. Grummit, S., "Early-Age Intrusion of Chloride Ions into Slag Cement Concrete," undergraduate thesis, University of Queensland, Brisbane, Australia, 1990.

9. McPolin, D.; Basheer, P. A. M.; Long, A. E.; Grattan, K. T. V.; and Sun, T., "Obtaining Progressive Chloride Profiles in Cementitious Materials," *Construction and Building Materials*, V. 19, No. 9, 2005, pp. 666-673.

10. Crank, J., *The Mathematics of Diffusion*, Oxford Science Publications, Clarendon Press, Oxford, 1956, 347 pp.

11. Collepardi, M.; Marcialis, A.; and Turrizani, R., "Penetration of Chloride Ions into Cement Pastes and Concretes," *Journal of American Ceramic Research Society*, V. 55, No. 10, 1972, pp. 534-535.

12. Tikalsky, P. J.; Pustka, D.; and Marek, P., "Statistical Variations in Chloride Diffusion in Concrete Bridges," *ACI Structural Journal*, V. 102, No. 3, May-June 2005, pp. 481-486.

13. Weyers, R. E., "Service Life Model for Concrete Structures in Chloride Laden Environments," *ACI Materials Journal*, V. 95, No. 4, July-Aug. 1998, pp. 445-453.

14. Suryavanshi, A. K.; Swamy, R. N.; and Cardew, G. E., "Estimation of Diffusion Coefficients for Chloride Ion Penetration into Structural Concrete," *ACI Materials Journal*, V. 99, No. 5, Sept.-Oct. 2002, pp. 441-449.

15. Thomas, M. D. A., and Matthews, J. D., "Performance of PFA Concrete in a Marine Environment—10-Year Results," *Cement and Concrete Composites*, V. 26, No. 1, 2004, pp. 5-20.

16. Nokken, M.; Boddy, A.; Hooton, R. D.; and Thomas, M. D. A., "Time Dependent Diffusion in Concrete—Three Laboratory Studies," *Cement and Concrete Research*, V. 36, No. 1, 2006, pp. 200-207.

17. Mangat, P. S., and Molloy, B. T., "Prediction of Long Term Chloride Concentration in Concrete," *Materials and Structures/Materiaux et Constructions*, V. 27, No. 170, 1994, pp. 338-346.

18. Alonso, M. C., and Sanchez, M., "Analysis of the Variability of Chloride Threshold Values in the Literature," *Materials and Corrosion*, V. 60, No. 8, 2009, pp. 631-637.

19. Glass, G. K., and Buenfeld, N. R., "The Presentation of the Chloride Threshold Level for Corrosion of Steel in Concrete," *Corrosion Science*, V. 39, No. 5, 1997, pp. 1001-1013.

20. Oh, B. H., and Jang, B. S., "Chloride Diffusion Analysis of Concrete Structures Considering Effects of Reinforcements," *ACI Materials Journal*, V. 100, No. 2, Mar.-Apr. 2003, pp. 143-149.

21. Ann, K. Y., and Song, H.-W., "Chloride Threshold Level for Corrosion of Steel in Concrete," *Corrosion Science*, V. 49, No. 11, 2007, pp. 4113-4133.